Excitation Spectrum and Effective Mass of the Even-Fraction Quantum Hall Liquid

Masaru Onoda,[1] Takahiro Mizusaki,[2] Takaharu Otsuka,[2,3] and Hideo Aoki[2]
[1]*High Energy Accelerator Research Organization (KEK), Tanashi Branch, Tokyo 188-8501, Japan*
[2]*Department of Physics, University of Tokyo, Hongo, Tokyo 113-0033, Japan*
[3]*RIKEN, Hirosawa, Wako-shi, Saitama 351-0198, Japan*
(Received 18 November 1999)

To probe the nature of the even-fraction quantum Hall system, we have investigated the low-lying excitation spectrum by exact diagonalization for finite systems. We have found (i) a striking one-to-one correspondence (i.e., a shell structure) between the spectrum and those for free (composite) fermions, (ii) a surprisingly straight scaling plot for the excitation energy that gives a zero gap (metal) in the thermodynamic limit, (iii) the effective mass evaluated from the scaling becoming heavier for $\nu = 1/2, 1/4, 1/6$, but (iv) some deviations from the single-mode or the Hartree-Fock composite fermion approximation.

PACS numbers: 73.40.Hm

In the physics of the fractional quantum Hall system, the composite fermion (CF) picture [1] not only serves as an illuminating way of understanding Laughlin's incompressible quantum liquid for the odd-fraction Landau level filling, ν, but also poses an interesting question of what is the nature at even fractions, which is the accumulation point of the fractional quantization. A seminal paper by Halperin, Lee, and Read [2] suggested that the system at $\nu = 1/2$ should be a Fermi liquid of CF's in the mean-field picture, which led to intensive studies. In contrast to the incompressible quantum Hall state or superconductors where energy gaps arise from many-body effects, we have to question here how the gap vanishes (i.e., how the liquid becomes compressible) despite the presence of the electron correlation.

Naively a CF, composed of an electron and an even number ($\tilde{\phi} = 2, 4, \ldots$) of flux quanta, feels the mean magnetic field $B_{\text{eff}} = (\nu^{-1} - \tilde{\phi})\phi_0\rho$, where $B = \nu^{-1}\phi_0\rho$ is the external magnetic field, ρ is the number density of electrons, and $\phi_0 \equiv 2\pi/e$ is the flux quantum (in units in which $c = 1$ and $\hbar = 1$). Thus B_{eff} vanishes for $\nu = 1/\tilde{\phi}$. There is, however, no guarantee that the mean field should be good, and the above argument does not, in fact, say anything as to where the electron-electron repulsion comes in. Recent developments [3–5] have indicated that we can define a "dipole" (composite particle + a correlation hole), where the flux attachment is thought to mimic the repulsive correlation of electrons. The Halperin-Lee-Read prediction on $\nu = 1/2$ has been reexamined in the dipole picture, and the compressible nature is reproduced [6].

These approaches still adopt mean-field treatments, and their validity has yet to be fully clarified. The difficulty arises because fluctuations of the Chern-Simons gauge field that implements the flux attachment should be significant. The fluctuations, in fact, determine the residual interaction between CF's as well as the effective mass, m^*, of a CF, which are difficult to evaluate analytically. Hence exact numerical studies for finite systems are valuable. Rezayi and Read [7] have numerically shown that the ground state for the $\nu = 1/2$ system on a sphere has the same angular momentum as expected from Hund's second rule for the same number of fermions in $B = 0$. Morf and d'Ambrumenil [8] have estimated m^* from the size scaling of the ground-state energy. However, we are still some way from understanding to what extent the CF picture applies.

One direct way going beyond the ground state is to look at the low-lying excitation spectrum—here we question whether or not there is a *one-to-one correspondence*, in the structure of the excitation spectrum, between the $\nu = 1/2$ liquid and a free fermion system in $B = 0$. This can also enable us to extract, through the size scaling of the energy gap, the effective mass. This is exactly the motivation of the present work.

There are two points we wish to make: (i) How to perform the size scaling is always a subtle problem, especially so when detecting the excitation gap that may vanish in the thermodynamic limit. (ii) Some analytic studies [2,9] have indicated that the nature of the $\nu = 1/2$ liquid is affected by the range of the electron-electron interaction. So we have taken a specific scaling sequence, and also varied the range in monitoring the excitation spectrum.

We shall show that (i) we do have a striking one-to-one correspondence between the interacting and free systems. The shell structure in the spectrum is deformed with the range of the interaction, which is interpreted here in terms of the single-mode approximation (SMA). (ii) The effective mass becomes heavier as ν is decreased as $\nu = 1/2 \rightarrow 1/4 \rightarrow 1/6$, where the increase in m^* is somewhat slower than the Hartree-Fock (HF) prediction of $m^*_{\text{HF}} \propto 1/\nu^2$.

We adopt the edge-free spherical system following Haldane [10,11], which has an extra virtue that the full rotational symmetry can be exploited in classifying the states. Dirac's quantization condition dictates that the total flux $4\pi R^2 B$ be an integral ($2S$) multiple of the flux quantum, where R is the radius of the sphere. The eigenvalue of the noninteracting part of the Hamiltonian is $\varepsilon = [l(l + 1) - S^2]/(2mR^2)$, where l ($\geq S$) is an integer.

 0031-9007/00/84(17)/3942(4)$15.00

The lowest Landau level (LLL) corresponds to $l = S$ with the Landau level filling given by $\nu = (N-1)/2S$ for N electrons. The electron-electron interaction, which is the whole Hamiltonian if only the LLL is considered, is given, up to a constant, as

$$\mathcal{H} = \frac{e^2}{2\ell\sqrt{S}} \sum_{J=0}^{2S} \sum_{M=-J}^{J} V_J d_{JM}^{\dagger} d_{JM} . \qquad (1)$$

Here $\ell \equiv 1/\sqrt{eB}$ is the magnetic length, $d_{JM}^{\dagger} \equiv \sum_{m_1,m_2} \langle Sm_1; Sm_2|JM\rangle c_{m_1}^{\dagger} c_{m_2}^{\dagger}$ where $c_m^{\dagger}/c_m$ creates or annihilates the mth orbit ($-S \le m \le S$) with $\langle j_1 m_1; j_2 m_2|JM\rangle$ being the Clebsch-Gordan coefficient, and the interaction matrix element is Haldane's LLL projected pseudopotential with $V_J \equiv 2\left[\begin{smallmatrix}4S-2J\\2S-J\end{smallmatrix}\right]\left[\begin{smallmatrix}4S+2J+2\\2S+J+1\end{smallmatrix}\right]/\left[\begin{smallmatrix}4S+2\\2S+1\end{smallmatrix}\right]^2$ for the Coulombic interaction.

For later reference let us look at the spectrum for free fermions in zero magnetic field, which is the mean-field solution for CF's at $\nu = 1/2$. The energy of a free fermion on a sphere is readily given by $\varepsilon = l(l+1)/(2m^*R^2)$, where l is the angular momentum and m^* the fermion's mass. We have to note that, with each level being $(2l+1)$-fold degenerate, a "closed shell" configuration is realized when $N = (l_F+1)^2$ [Fig. 1(a)]. Here l_F ($= 1, 2, 3, \ldots$ for $N = 4, 9, 16, \ldots$) is the highest occupied l, so that we may call this the Fermi angular momentum in analogy with the Fermi momentum in the planar system.

When $N \neq (l_F+1)^2$, the ground state of the noninteracting system is thus degenerate, or has an "open shell." For interacting particles the degeneracy is lifted, and the total angular momentum of the ground state becomes nonzero [7]. Since this can obscure the scaling, a straightforward way is to concentrate on the closed-shell sequence satisfying $N = (l_F+1)^2 = 4, 9, 16, \ldots$. For this sequence the total angular momentum of the ground state remains zero, and provides a natural sequence toward the infinite system for establishing both the structure of the low-lying excitation spectrum and the energy gap.

The simplest class of excitations from a closed shell is "single-exciton" excitations where a particle is ejected from the l_Fth shell to the (l_F+1)th, as has been pointed out by Rezayi and Read [7]. The exciton's angular momentum takes the values $L = 1, \ldots, 2l_F+1$. These excitations (abbreviated here as $[l_F] \to [l_F+1]$) provide the lowest-lying branch for $1 \le L \le 2l_F+1$.

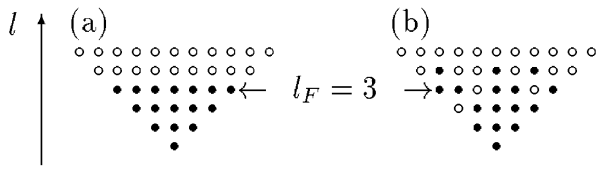

FIG. 1. (a) A closed-shell ground state of the $N = 16$ free system. Solid (open) circles represent occupied (empty) states. (b) An example of multiexciton excitations ($[l_F-1][l_F]^2 \to [l_F+1]^3$ here).

We can generalize this, including *multiple excitons*, to obtain the whole picture. For $2l_F+1 < L \le 4l_F$, the lowest-lying excitations are $[l_F]^2 \to [l_F+1]^2$, i.e., two-exciton excitations. For $4l_F < L \le 6l_F-3$ for $N \ge 9$ $[l_F]^3 \to [l_F+1]^3$ and so on, where n-exciton excitations $[l_F]^n \to [l_F+1]^n$ exist for $L \le n(2l_F+2-n)$. Overall, however, the lowest-lying states for $L \lesssim 6l_F$ are one, two, and three excitons, whose energies Δ_ε form *steps* moving up at $L_{\mathrm{MAX}} \simeq 2l_F, 4l_F, 6l_F$, respectively, as indicated (□) in Fig. 2 for $N = 16$, although there are finite-size corrections in $L_{\mathrm{MAX}} = 2l_F+1, 4l_F, 6l_F-3$ as we have mentioned.

Having looked at the free case, we now come to the structure of low-lying excitations in the interacting system. The exact low-lying energies are obtained by diagonalizing the Hamiltonian matrix. For $\nu = 1/2$ we have $2S = 2(N-1)$, and the dimension of the Hamiltonian is 4 669 367 in the $L_z = 0$ subspace for $N = 16$ electrons. The Lanczos diagonalization method with a parallel processing is employed. If we explore the spectra for $N = 16$ (Fig. 2) and its evolution from $N = 4$ (not shown) and $N = 9$ (Fig. 5 below), we are led to a well-defined series of cusps in the excitation spectrum, whose positions *exactly* agree with the predicted positions for the free fermions at $L_{\mathrm{MAX}} \simeq 2l_F, 4l_F, 6l_F$, etc. [12]. The degeneracies (flatness of the steps) in the latter case are naturally lifted due to the interaction between CF's, but the effect of interaction turns out to be weak enough to preserve the shell structure, which remarkably persists up to the angular momentum as large as 30. This is the first key finding in this Letter. For $L \ge 6l_F-2$, complicated excitations such as $[l_F-1]^m[l_F]^n \to [l_F+1]^{m'}[l_F+2]^{n'}$ ($m+n = m'+n'$) become the lowest excitation of the free system, which continues to agree with the numerical result.

We can next evaluate the energy gap, Δ. In the free fermion system, the lowest excitation corresponds to $[l_F] \to [l_F+1]$ with $\Delta \equiv (l_F+1)/(m^*R^2)$. This quantity has a well-defined scaling, $\Delta = (4\pi\rho/m^*)[\sqrt{N}/(N-1)]$ when N is varied with ρ fixed. For the

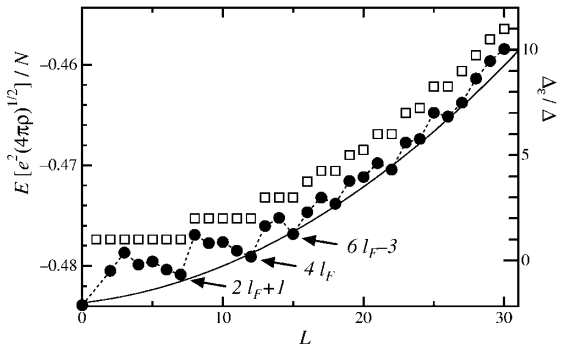

FIG. 2. Low-lying excitation spectrum for $N = 16$ (solid circles). The dashed line is a guide for the eye, while the full curve represents $\propto L(L+1)$. The low-lying excitation spectrum Δ_ε for free fermions is also shown (□).

interacting system, the cusped structure revealed here enables us to identify the position of the lowest excited state, which always occurs as the first cusp at $L = 2l_F + 1$ (the high-L end of the single-exciton excitation). Figure 3 shows this gap for $\nu = 1/2$ [13]. We can immediately see a surprisingly accurate linear scaling that extrapolates to zero for $N \to \infty$ if we take $\sqrt{N}/(N-1)$ as the scaling variable, as guided by the free-system behavior, $\Delta = (4\pi\rho/m^*)[\sqrt{N}/(N-1)]$.

This same formula can be used to extract the effective mass m^* of CF's from the gradient of the scaling plot, with the result $1/m^* = (0.185 \pm 0.002)e^2\ell$. The $1/m^*$ obtained here from the excitation gap is slightly smaller than $1/m^* \simeq (0.2 \pm 0.02)e^2\ell$, estimated from the ground-state energy per particle [8]. On the other hand, the present value is slightly larger than the analytic estimate, $1/m^* \simeq e^2\ell/6$, obtained from the interaction energy between an electron and a correlation hole in the first-quantized picture [5] or the self-energy of the CF in the temporal gauge in the HF approximation [14].

The effect of the gauge fluctuations can be probed by how the gap and mass depend on the number of flux quanta attached ($\tilde{\phi}$), so we further obtained the scaling plot for the sequence $\nu = 1/\tilde{\phi} = 1/2, 1/4, 1/6$ in Fig. 3 [15]. The gap again vanishes linearly for $N \to \infty$ (Fig. 3), where the effective mass systematically becomes heavier with $\tilde{\phi}$ as shown in Fig. 4 for $N = 9$. In the HF approximation for the CF we can show [16] that m^* should scale as

$$\frac{1}{m^*_{\rm HF}(\tilde{\phi})} = \frac{1}{6}\left(\frac{2}{\tilde{\phi}}\right)^2 \frac{e^2}{\sqrt{4\pi\rho}}. \qquad (2)$$

This is a decreasing function of $\tilde{\phi}$ as well, but the present numerical result is seen to deviate from the HF result (inset of Fig. 4) for larger $\tilde{\phi}$ [17].

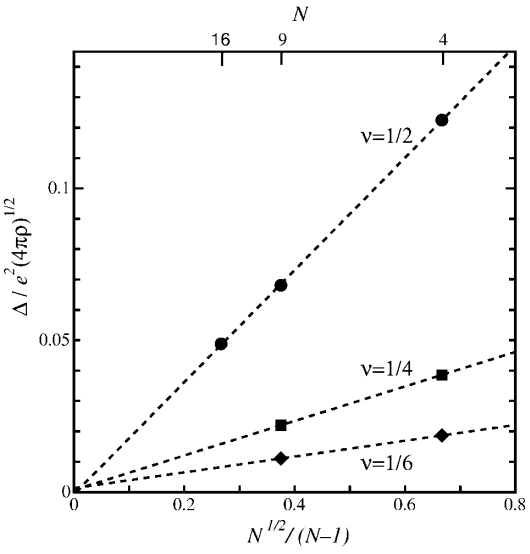

FIG. 3. Size scaling of the gap for $\nu = 1/2, 1/4, 1/6$. The dashed lines are linear fit to the data.

Now let us look more closely at the excitation spectra. Note in passing that the overall shape of the spectrum exhibits an $\propto L^2$ asymptote as evident from Fig. 2. We can explain this by converting the Hamiltonian in the $c^\dagger c^\dagger cc$ form to $c^\dagger cc^\dagger c$. We have then, up to a constant, $e^2/(2\ell\sqrt{S})\sum_{K=1}^{2S}\tilde{V}_K\rho_K\cdot\rho_K$ where $\rho_K\cdot\rho_K \equiv \sum(-1)^M\rho_{KM}\rho_{K,-M}$ and $\rho_{KM} \equiv \sum(-)^{S+m_2}\langle Sm_1; Sm_2|KM\rangle c^\dagger_{m_1}c_{-m_2}$. The transformed coefficient becomes $\tilde{V}_K \equiv \sum_{J=0}^{2S}(-1)^{2S+J}(2J+1)\{^{SSJ}_{SSK}\}V_J$, where $\{^{SSJ}_{SSK}\}$ is Wigner's $6j$ symbol. In this representation, ρ_{1M} is nothing but the (LLL projected) total angular momentum operator, so the leading term becomes $\rho_1\cdot\rho_1 = [3/S(S+1)(2S+1)]\hat{\mathbf{L}}\cdot\hat{\mathbf{L}}$, which explains the asymptote $\propto L(L+1)$.

Now we come to what happens when the range of interaction is changed. We have calculated the excitation spectra replacing the pseudopotential V_{2S-m} with $(V_{2S-m})^a$. Since V_{2S-m} is the potential between two electrons with the relative angular momentum m, $a < 1$ ($a > 1$) corresponds to the interaction longer (shorter) ranged than Coulombic.

The numerical result in Fig. 5 [12] shows that the cusped structure in the spectra becomes more pronounced (i.e., effect of the inter-CF interaction becomes enhanced) as the interaction is made shorter ranged, although the positions of cusps remain the same. So the free CF picture seems to be better for longer-ranged interaction. This is in sharp contrast with the Laughlin's liquid at odd denominators for which the mean-field CF picture yields even an exact ground state when the interaction is short ranged enough. The cusps sticking to $2l_F, 4l_F, \ldots$ remind us of the Tomonaga-Luttinger (TL) liquid, a totally different system in one dimension, where the cusps, having a topological origin, do not change with the form of interaction, either.

The tendency that the system lies farther away from the Fermi liquid for shorter-ranged interactions is consistent with analytic studies. Namely, an improved random-phase approximation [2] and a renormalization group study [9] suggest that for short-ranged potentials the one-particle Green's function has a branch cut rather than a pole just as in the TL liquid. For a longer-ranged case the

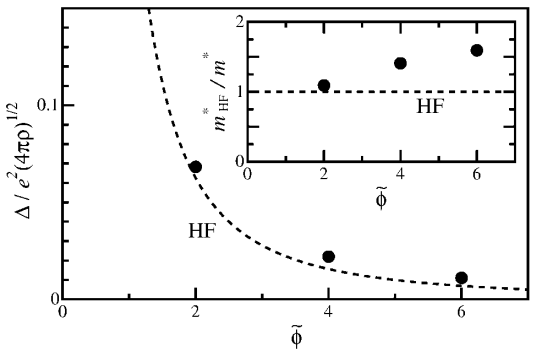

FIG. 4. Δ ($\propto 1/m^*$) versus $\nu = 1/\tilde{\phi} = 1/2, 1/4, 1/6$ for $N = 9$. The dashes lines represent the HF result, with the inset depicting $m^*_{\rm HF}/m^*$.

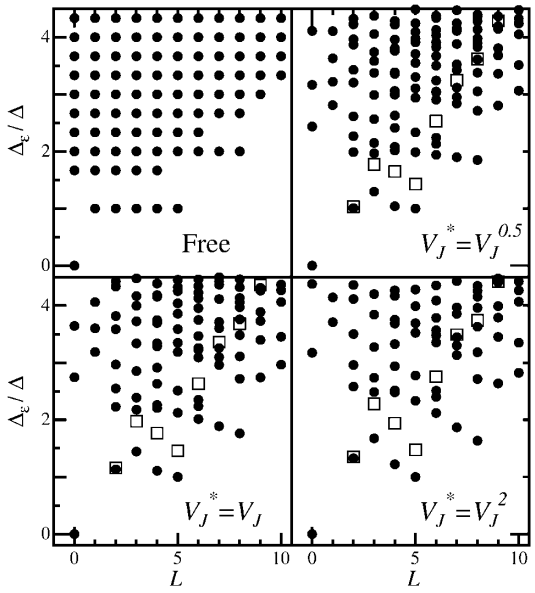

FIG. 5. Full excitation spectra for $\nu = 1/2$ with $(V_{2S-m})^a$ ($a = 0.5, 1.0, 2.0$) for $N = 9$ ($l_F = 2$). The energy is normalized by the gap at $L = 2l_F + 1 (= 5)$ for each value of a. The SMA result is also shown (□).

Fermi-liquid properties are recovered. To test these predictions from numerical low-lying spectra will require further investigations, including correlation function studies. However, we can compare the behavior of the lowest cusp (i.e., single-exciton branch) with the SMA, where the ρ_{LM} defined above operated on the ground state $|\Psi_0\rangle$ is used as the trial function in evaluating the energy, $\langle\Psi_0|\rho_{LM}^\dagger(H - E_0)\rho_{LM}|\Psi_0\rangle/\langle\Psi_0|\rho_{LM}^\dagger\rho_{LM}|\Psi_0\rangle = f(L)/s(L)$. The SMA result (□ in Fig. 5) roughly reproduces the gradient of the branch, although we encounter a deviation larger than those in the odd-fraction liquids. We can numerically show that the structure factor $s(L)$ remains almost identical as the interaction range is varied, so the change in the oscillator strength $f(L)$ is dominating the shape of the cusp.

To summarize, the present numerical result, done on the largest scale currently available, has enabled us to show that the gauge fluctuations in the even-fraction metals are substantial, but not so strong as to destroy the shell structure in the low-lying excitation spectrum. We are also extending the present study to the spin degrees of freedom, which will be published elsewhere.

We acknowledge Peter Maksym for a critical reading of the manuscript, and Kazuhiko Kuroki for illuminating discussions. This work was supported in part by Grants-in-Aid for Scientific Research (A211125206) and (A210304019) from the Japanese Ministry of Education. The parallel computing has been done on the Alphleet in RIKEN.

[1] J. K. Jain, Phys. Rev. Lett. **63**, 199 (1989); Phys. Rev. B **40**, 8079 (1989); **41**, 7653 (1990); Adv. Phys. **41**, 105 (1992); Surf. Sci. **263**, 65 (1992); A. Lopez and E. Fradkin, Phys. Rev. B **44**, 5246 (1991).

[2] B. I. Halperin, P. A. Lee, and N. Read, Phys. Rev. B **47**, 7312 (1993). See also B. L. Altshuler, L. B. Ioffe, and A. J. Millis, Phys. Rev. B **50**, 14 048 (1994).

[3] N. Read, Phys. Rev. Lett. **62**, 86 (1989); Surf. Sci. **361/362**, 7 (1996); Phys. Rev. B **58**, 16 262 (1998).

[4] R. Rajaraman and S. L. Sondhi, Int. J. Mod. Phys. B **10**, 793 (1996).

[5] R. Shankar and G. Murthy, Phys. Rev. Lett. **79**, 4437 (1997).

[6] A. Stern, B. I. Halperin, F. von Oppen, and S. H. Simon, Phys. Rev. B **59**, 12 547 (1999).

[7] E. Rezayi and N. Read, Phys. Rev. Lett. **72**, 900 (1994).

[8] R. Morf and N. d'Ambrumenil, Phys. Rev. Lett. **74**, 5116 (1995).

[9] C. Nayak and F. Wilczek, Nucl. Phys. **B417**, 359 (1994); **B430**, 534 (1994); S. Chakravarty, R. E. Norton, and O. F. Syljuåsen, Phys. Rev. Lett. **74**, 1423 (1995); I. Ichinose and T. Matsui, Nucl. Phys. **B441**, 483 (1995); M. Onoda, I. Ichinose, and T. Matsui, *ibid.* **B446**, 353 (1995).

[10] F. D. M. Haldane, Phys. Rev. Lett. **51**, 605 (1983).

[11] G. Fano, F. Ortolani, and E. Colombo, Phys. Rev. B **34**, 2670 (1986).

[12] For $L = 1$ single-exciton states cannot be constructed as shown by SMA [7], so we have excluded the $L = 1$ result in Fig. 2, but included it in Fig. 5.

[13] For $N = 4$ and $\nu = 1/2$, the lowest state has $L = 2$, but we have plotted the slightly different energy for $L = 3 (= 2l_F + 1)$ to compare with the $N = 9, 16$ results for which the lowest excitations have $L = 2l_F + 1$.

[14] Y. Yu, Z. Su, and X. Dai, Phys. Rev. B **57**, 9897 (1998).

[15] The dimension of the Hamiltonian for $\nu = 1/6, N = 9$ is about 20×10^6, which is as far as we can treat with parallel processing.

[16] Reference [14] also reports the HF mass, but the factor involving $\tilde{\phi}$ is not explicitly included.

[17] There are few experimental estimates of m^* for $\nu = 1/4$; an early result [R. R. Du *et al.*, Phys. Rev. Lett. **70**, 2944 (1993)] indicates a heavier mass for $\nu = 1/4$ than in $\nu = 1/2$.